THE JOURNAL OF BIOLOGICAL CHEMISTRY Vol. 278, No. 47, Issue of November 21, pp. 47291–47298, 2003
Printed in U.S.A.

Oscillatory Shear Stress Stimulates Endothelial Production of O_2^- from p47^{phox}-dependent NAD(P)H Oxidases, Leading to Monocyte Adhesion*

Received for publication, May 16, 2003, and in revised form, August 20, 2003
Published, JBC Papers in Press, September 4, 2003, DOI 10.1074/jbc.M305150200

Jinah Hwang‡§, Aniket Saha‡§, Yong Chool Boo‡, George P. Sorescu‡, J. Scott McNally¶, Steven M. Holland‖, Sergei Dikalov¶, Don P. Giddens‡, Kathy K. Griendling¶, David G. Harrison¶, and Hanjoong Jo‡¶**

From the ‡Wallace H. Coulter Department of Biomedical Engineering, Georgia Institute of Technology and Emory University and the ¶Division of Cardiology, Emory University, Atlanta, Georgia 30322 and ‖the Laboratory of Host Defenses, NIAID, National Institutes of Health, Bethesda, Maryland 20892

Arterial regions exposed to oscillatory shear (OS) in branched arteries are lesion-prone sites of atherosclerosis, whereas those of laminar shear (LS) are relatively well protected. Here, we examined the hypothesis that OS and LS differentially regulate production of O_2^- from the endothelial NAD(P)H oxidase, which, in turn, is responsible for their opposite effects on a critical atherogenic event, monocyte adhesion. We used aortic endothelial cells obtained from C57BL/6 (MAE-C57) and p47$^{phox-/-}$ (MAE-p47$^{-/-}$) mice, which lack a component of NAD(P)H oxidase. O_2^- production was determined by dihydroethidium staining and an electron spin resonance using an electron spin trap methoxycarbonyl-2,2,5,5-tetramethyl-pyrrolidine. Chronic exposure (18 h) to an arterial level of OS (± 5 dynes/cm^2) increased O_2^- (2-fold) and monocyte adhesion (3-fold) in MAE-C57 cells, whereas chronic LS (15 dynes/cm^2, 18 h) significantly decreased both monocyte adhesion and O_2^- compared with static conditions. In contrast, neither LS nor OS were able to induce O_2^- production and monocyte adhesion to MAE-p47$^{-/-}$. Treating MAE-C57 with a cell-permeable superoxide dismutase compound, polyethylene glycol-superoxide dismutase, also inhibited OS-induced monocyte adhesion. In addition, over-expressing p47^{phox} in MAE-p47$^{-/-}$ restored OS-induced O_2^- production and monocyte adhesion. These results suggest that chronic exposure of endothelial cells to OS stimulates O_2^- and/or its derivatives produced from p47^{phox}-dependent NAD(P)H oxidase, which, in turn, leads to monocyte adhesion, an early and critical atherogenic event.

Fluid shear stress, the frictional force generated by blood flow over the vascular endothelium, is a major factor in atherogenesis. The importance of shear stress in vascular biology and pathophysiology has been highlighted by the focal development patterns of atherosclerosis in hemodynamically defined regions. For example, regions of branched and curved arteries experience disturbed blood flow patterns, including oscillatory shear stress (OS),[1] typically ranging ± 5 dynes/cm^2 (± indicates changes in flow directions) (1, 2). These disturbed shear regions correspond to "lesion-prone" areas that develop early forms of atherosclerotic lesions (1–3). In contrast, relatively straight arteries, which are exposed to steady uni-directional laminar shear stress (typically ranging from 5–25 dynes/cm^2), are usually protected from early atherosclerotic plaque development (1, 2). The mechanisms by which laminar shear (LS) acts as atheroprotective force whereas OS initiates or contributes to atherogenesis have been the subject of intense investigation by many researchers.

The vascular endothelium is in direct contact with blood flow and acts as a mechanotransducer by sensing and transducing the changes in local mechanical forces into cellular signals. Endothelial function, shape, physiology, and pathophysiology are greatly regulated by the types (uni-directional laminar or disturbed flow conditions) and magnitudes (high or low) of the shear stress imparted upon them (4, 5).

LS exerts atheroprotective effects, including regulation of vascular tone, diameter and vessel wall remodeling, prevention of apoptosis, and monocyte adhesion (4, 5). These functions are mediated by regulating the production of several vasoactive factors, including NO, and by the expression of mechanosensitive and atheroprotective genes in endothelial cells (4–6). In contrast, the exposure of endothelial cells to disturbed flow conditions such as OS has been shown to induce several inflammatory and pro-atherogenic responses, including monocyte adhesion as observed in human arteries, animal models, and cultured endothelial cells (4, 7, 8, 34). The induction of inflammatory adhesion molecules, including E-selectin, vascular cell adhesion molecule-1 (VCAM-1), and intercellular adhesion molecule-1 (ICAM-1) and the consequent monocyte adhesion to the lesion-prone areas seem to be the earliest visible markers leading to atherosclerotic plaque development (3, 7, 8, 34–36).

Reactive oxygen species (ROS), including superoxide (O_2^-), hydrogen peroxide (H_2O_2), and peroxynitrite ($ONOO^-$), have been implicated in atherogenesis (9, 10). Although the phagocytic NAD(P)H oxidase is the major source of O_2^- in the circulatory system, vascular endothelial cells, smooth muscle cells,

* This work was supported by National Institutes of Health Grants HL71014 and HL67413 (to H. J.) and NASA Grant NAG2-1348 (to H. J.). The costs of publication of this article were defrayed in part by the payment of page charges. This article must therefore be hereby marked "*advertisement*" in accordance with 18 U.S.C. Section 1734 solely to indicate this fact.

§ These authors contributed equally to this publication.

** To whom correspondence should be addressed. Tel.: 404-712-9654; Fax: 404-727-3330; E-mail: hanjoong.jo@bme.gatech.edu.

[1] The abbreviations used are: OS, oscillatory shear; LS, laminal shear; NO, nitric oxide; ROS, reactive oxygen species; DiI-Ac-LDL, 1,1′-dioctadecyl-3,3,3,3′-tetramethyl-indocarbocyanine perchlorate-labeled acetylated low density lipoprotein; DHE, dihydroethidium; CMH, methoxycarbonyl-2,2,5,5-tetramethyl-pyrrolidine; PEG, polyethylene glycol; SOD, superoxide dismutase; TBAP, tetrakis-(4-benzoic acid) porphyrin.

and fibroblasts also express functional leukocyte-type NAD(P)H oxidases (9). The endothelial NAD(P)H oxidase is comprised of five major components, namely $gp91^{phox}$ (and/or its homologues) and $p22^{phox}$ in the membrane and $p47^{phox}$, $p67^{phox}$, and Rac in the cytosol, and it has been suggested to be the major source of O_2^- in these cells (9). $p47^{phox}$ in endothelial cells has been shown to play an essential role in activation of NAD(P)H oxidase and the production of O_2^- (11, 12).

Recent results have shown that both LS and OS can induce ROS production from endothelial cells (13, 14). De Keulenaer *et al.* suggested that an NAD(P)H-dependent oxidase was activated by LS and OS (14); however, the molecular identity of this oxidase remains to be determined. Moreover, the identity of its source as well as its pathophysiological roles in cells remain unclear due, in large part, to the lack of specific molecular approaches, thus relying heavily on the use of inhibitors/scavengers of ROS. For example, chronic exposure to OS has been shown to activate endothelial cells to stimulate monocyte adhesion, which can be blocked by treating with a nonspecific antioxidant, *N*-acetylcysteine, during shear (8). This result suggests a role for ROS in this inflammatory response.

Here, we hypothesized that the ROS produced by shear stress is O_2^- derived from NAD(P)H oxidase. We further hypothesized that LS and OS differentially regulate production of O_2^-, which, in turn, is responsible for regulating monocyte adhesion. To examine these hypotheses, we used aortic endothelial cells (MAE cells) obtained from either normal (C57BL/6) or knockout mice ($p47^{phox-/-}$) that lack a key component of NAD(P)H oxidases, the $p47^{phox}$ gene (15). Our results demonstrate that the chronic exposure of endothelial cells to OS stimulates monocyte adhesion by a mechanism dependent on O_2^- derived from NAD(P)H oxidase, whereas LS induces transient O_2^- production followed by a substantial inhibition in both O_2^- production and monocyte adhesion.

MATERIALS AND METHODS

Genotyping of $p47^{phox}$ DNA—Genotyping of mice was performed with the $p47^{phox}$-specific primers 5′-ACATCACAGGCCCCATCATCCTCC-3′ and 5′-GGAGAGCCCCCTTTCTCTCCCTCA-3′ and the neomycin-resistant primer 5′-CAACGTCGAGCACAGCTGCGCAAG-3′ (15). PCR was performed in a 50-μl reaction containing 200 μM dNTP, 1.5 mM $MgCl_2$, 10 mM Tris-HCl, pH 8.3, 2 units of *Taq* polymerase (Invitrogen), and 0.5 μM each primer. The denaturing temperature was 95 °C for 3 min, and the cycling parameters were 95 °C for 30 s, 60 °C for 30 s, and 72 °C for 1 min for 30 cycles. PCR products were analyzed by agarose gel (2%) electrophoresis.

Isolation and Culture of Mouse Thoracic Aorta Endothelial Cells—Pathogen-free male C57BL/6 mice were purchased from the Jackson Laboratories, and $p47^{phox-/-}$ mice were described previously (15). MAE cells were isolated by modifying a previously described method (16). Briefly, the thoracic aorta was dissected free of adventitia and cut into small pieces (~2 × 2 mm). The explants were cultured intimal side down on Matrigel (BD Biosciences)-coated 6-well plates in an initial growth medium (Dulbecco's modified Eagle's medium containing 20% fetal bovine serum, 100 μg/ml endothelial cell growth supplement (Sigma), 10 units/ml heparin, and 1% penicillin/streptomycin). Initially, a very small volume of medium was added onto the outside of the piece of aorta, which was just enough to keep the Matrigel wet but not enough to cover the outer side of the aorta; this inhibited fibroblast growth. One drop of medium was added each day. Two to three days post-isolation, endothelial cells began to grow out of the aortic intima. Aortic pieces were removed from the wells showing capillary-like tubes within 4–5 days, a characteristic of endothelial cells on Matrigel matrix. Adherent cells were allowed to grow in 2 ml of medium. After ~10 days of culture, cells grown out of the explants were trypsinized and seeded on collagen-coated 6-well tissue culture plates.

Cell Sorting and Characterization—To isolate pure MAE cells, wells containing cells reaching confluence with apparent cobblestone shapes were loaded with acetylated low density lipoprotein conjugated to 1,1′-dioctadecyl-3,3,3,3′-tetramethyl-indocarbocyanine perchlorate (DiI-Ac-LDL) and sorted by fluorescence-activated cell sorting. Briefly, cells were incubated with 10 μg/ml DiI-Ac-LDL (Biomedical Technologies) in the initial growth medium for 4 h at 37 °C. The cells were rinsed with the initial growth media, trypsinized, and centrifuged for 5 min at 1,000 rpm. Cell pellets were resuspended into a single cell suspension in fresh medium and sorted by florescence-activated cell sorting (488-nm excitation and 525-nm emission wavelength). Rat vascular smooth muscle cells and bovine and mouse aortic endothelial cells were used as negative and positive controls, respectively. The sorted cells were grown on collagen-coated tissue culture plates and observed by fluorescent microscopy. Only when all of the observed cells were labeled with DiI-Ac-LDL were the cells used for further study.

To further ascertain the purity of endothelial cells, passaged endothelial cells were stained with a polyclonal von Willebrand factor antibody (Dako, 1:100 dilution) for 30 min, followed by rhodamine-conjugated goat anti-rabbit IgG antibody (Molecular Probes, 1:1000 dilution) for 30 min. Subsequently, cells were mounted with an anti-fade (Molecular Probes) and photographed with a Zeiss fluorescent microscope.

Cell Culture and Shear Exposure—MAE cells obtained from C57 (MAE-C57) and $p47^{phox-/-}$ (MAE-$p47^{-/-}$) mouse aortas were maintained at 37 °C and 5% CO_2 in a growth medium (the same as the initial growth medium except for the heparin concentration, 2.5 units/ml). Cells used in this study were between passages 4 and 10. For shear experiments, cells were plated on 0.5% gelatin-coated 100-mm plates (Falcon). One day prior to shear experiments, the media were changed to endothelial cell growth supplement-free growth media. Monocytes from a human monocytic leukemia cell line, THP-1, were obtained from the American Type Culture Collection and maintained at 37 °C and 5% CO_2 in a growth medium (RPMI 1640; Invitrogen) containing 10% fetal bovine serum, 2 mM L-glutamine, 50 μg/ml streptomycin, and 50 units/ml penicillin. Monocytes were maintained at a density of 5×10^5 cells/ml.

Confluent MAE monolayers grown in 100-mm tissue culture dishes were exposed to an arterial level of uni-directional laminar shear stress (15 dynes/cm^2) in the growth medium by rotating a Teflon cone (0.5° cone angle) as we have described previously (17). To mimic unstable shear conditions *in vivo*, cells were exposed to oscillatory shear stress with directional changes of flow at 1 Hz cycle (± 5 dynes/cm^2) by rotating the cone back-and-forth using a stepping motor (Servo Motor) controlled by a computer program (DC Motor Company) (7).

Determination of Protein Expression by Western Blot Analysis—Cell lysates (20 μg protein each) were resolved by 10% SDS-PAGE, transferred to a polyvinylidene difluoride membrane (Millipore), and probed with a primary antibody specific to $p47^{phox}$ (BD Transduction Laboratories). IgG conjugated with alkaline phosphatases (Bio-Rad) were used as secondary antibodies, and the membrane was developed using chemiluminescence detection (18). The intensities of the immunoreactive bands in the Western blots were quantified using the NIH IMAGE program.

Superoxide Measurement by Dihydroethidium—Intracellular O_2^- production was measured using the cell-permeable dye dihydroethidium (DHE; Molecular Probes), which binds to nuclear DNA when oxidized by O_2^- and emits red fluorescence (19, 20). Briefly, following shear exposure in the presence or absence of antioxidants, cells were immediately incubated with 10 μM DHE for 10 min at 37 °C. Cells were then washed in ice-cold fresh DHE-free medium, and the fluorescence intensity was semi-quantified by Bio-Rad laser scanning fluorescence microscopy (514-nm excitation line and 580 ± 30 nm band pass filter) (19). O_2^- production was estimated by determining the intensity of the fluorescence images taken randomly at a minimum of five different locations of each dish using the NIH IMAGE program (Scion Image Beta 4.02).

Superoxide Measurement by ESR—As a second approach, O_2^- was measured by ESR spectroscopy using the spin probe, methoxycarbonyl-2,2,5,5-tetramethyl-pyrrolidine (CMH), as described previously (21). Each ESR assay was carried out using cells treated with or without polyethylene glycol-superoxide dismutase (PEG-SOD; 50 units/ml) to quantify the SOD-inhibitable formation of CM$^\bullet$. Following experimental treatments (shear or static), MAE cells were rinsed with ice-cold Krebs-Hepes buffer (5.6 mM D-glucose, 2.5 mM $CaCl_2$, 99 mM NaCl, 4.69 mM KCl, 1.2 mM $MgSO_4$, 25 mM $NaHCO_3$, 1 mM KH_2PO_4, and 20 mM sodium-HEPES; pH 7.4) and scraped from the tissue culture dishes. To inhibit iron-catalyzed reactions, 25 μM desferrioxamine and 5 μM diethylenetriamine-pentaacetic acid were added to all samples. After centrifugation at 2,000 rpm for 1 min, the cells were resuspended in 200 μl of Krebs-Hepes buffer and stored on ice. Cells were counted, and an equal number of cells containing 1 mM CMH was transferred to a 50-μl capillary tube to scan in a super high Q microwave cavity of an EMX ESR spectrometer (Bruker BioSpin). The ESR settings were as follows: field sweep, 50 G; microwave frequency, 9.78 GHz; microwave power, 20

milliwatts; modulation amplitude, 2 G; conversion time, 656 ms; time constant, 656 ms; resolution, 512 points; and receiver gain, 1×10^5. The kinetics were recorded by using a 1312-ms conversion time and 5248-ms time constant and monitoring the ESR amplitude of the low field component of the ESR spectrum of 3-methoxycarbonyl-proxyl.

Monocyte Adhesion Assay—The monocyte binding to endothelial cells was determined using a modified method of Tsao *et al.* (22). Briefly, THP-1 cells (5×10^5 cells/ml) were labeled with the fluorescent dye 2′,7′-bis(carboxyethyl)-5(6)-carboxyfluorescein acetoxymethyl ester (BCECF-AM; Molecular Probes) (1 μg/μl) in serum-free RPMI medium for 45 min at 37 °C (8). Following exposure to shear stress or other treatments, the endothelial cells were washed in RPMI medium before adding 2′,7′-bis(carboxyethyl)-5(6)-carboxyfluorescein-loaded THP-1 cells (1:1 ratio). After a 30-min incubation at 37 °C under no-flow conditions, unbound monocytes were removed by washing the endothelial dishes five times with Hank's phosphate-buffered solution. Bound monocytes were quantified by either counting the cells under a fluorescent microscope or by measuring the fluorescent intensity of cell lysates by fluorescence spectrophotometry (8, 22). Both methods yielded similar results.

$p47^{phox}$ Transfection into MAE-$p47^{-/-}$—MAE-$p47^{-/-}$ cells were grown to 90% confluency and transfected with the full-length $p47^{phox}$ cDNA inserted in EbopLPP vector (kindly provided by Dr. B M. Babior) or the empty vector alone using LipofectAMINE as we have described previously (7). Following 36 h of incubation, the medium was changed to a fresh growth medium. Transfection efficiency (30–40%) was estimated by determining green fluorescent protein expression (pEGFP vector, Clontech) by fluorescent microscopy.

Statistical Analysis—For all the experiments, statistical analysis was performed by using the Student's *t* test. A significance of $p < 0.05$ from three or more independent experiments was considered statistically significant.

RESULTS

Characterization of MAE-C57 and MAE-$p47^{-/-}$ Cells—Genotypes of C57BL/6 and $p47^{phox-/-}$ mice were confirmed by PCR with genomic DNA obtained from tail tissues using two $p47^{phox}$-specific primers and neomycin-resistant primers as described (15). As expected, the wild type mice showed a 650-bp band (Fig. 1*A*, *lane 1*), whereas $p47^{phox}$ knockout mice showed a 900-bp band because it contains the neomycin cassette inserted to generate the knockout (Fig. 1*A*, *lane 2*). Fig. 1*A*, *lane 3* was a negative control for PCR containing no DNA.

To assess the purity of wild type MAE and MAE-$p47^{-/-}$ cells isolated from the thoracic aortas of C57BL/6 and $p47^{phox-/-}$ mice, cells were labeled with the endothelial marker DiI-Ac-LDL (Fig 1, *B* and *C*). The identity and purity of MAE cells were further confirmed by the positive staining of all sorted cells using an additional endothelial cell marker, the von Willebrand factor (Fig. 1*C*). Immunostaining with antibodies specific to the platelet endothelial cell adhesion molecule (PECAM-1) and endothelial nitric oxide synthase (eNOS) further confirmed endothelial cell purity (data not shown).

To ensure that the $p47^{phox}$ gene product was indeed absent in MAE-$p47^{-/-}$ cells, cell lysates were analyzed by Western blot using an antibody specific for $p47^{phox}$. As expected, MAE-$p47^{-/-}$ cells did not express $p47^{phox}$ protein in more than four independent preparations from four different mouse thoracic aortas, whereas its expression was clearly identified in more than four independent MAE-C57 cell preparations (Fig. 1*E*; see also Fig. 9*C*).

Alignment of MAE Cells by Shear Stress—MAE-C57 and MAE-$p47^{-/-}$ cells grown under static (no flow) culture conditions were not distinguishable from each other and showed typical cobblestone shapes (Fig. 2). Although we do not use cells beyond 10 passages for any of our studies, both cell types could be cultured for at least 10 passages without showing any detectable phenotypic changes. To examine whether these cells respond to shear stress in an expected manner, confluent MAE-C57 and MAE-$p47^{-/-}$ monolayers were exposed to arterial levels of LS or OS by using a cone-and-plate device for 18 h.

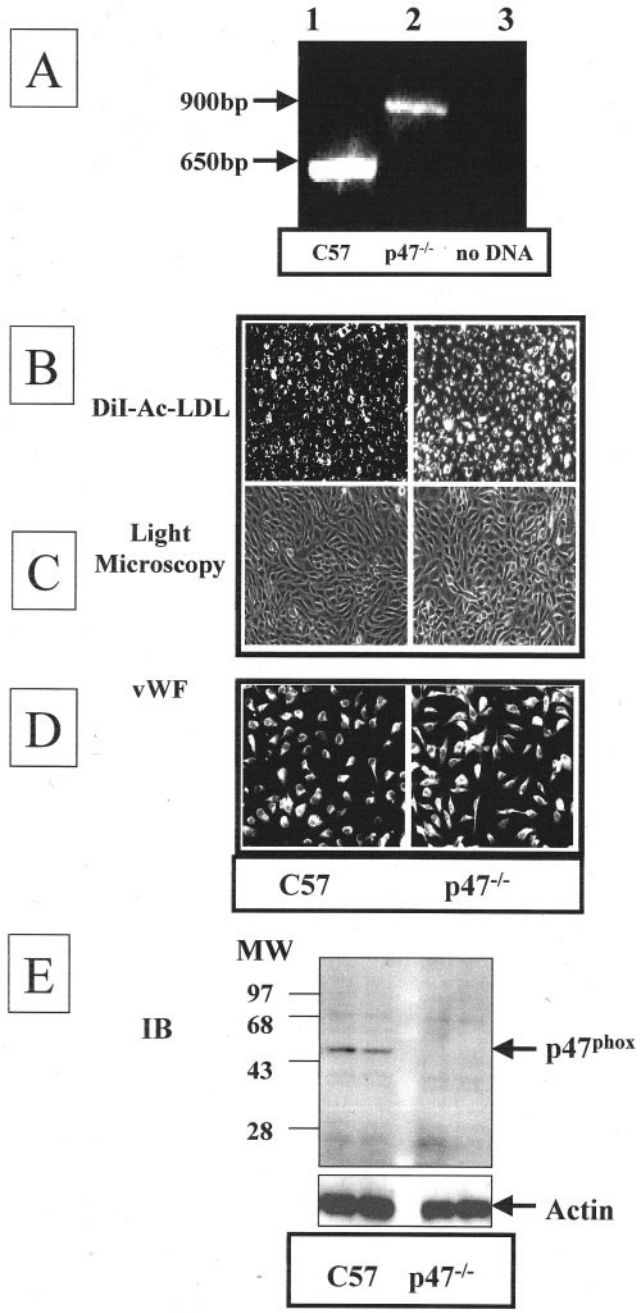

FIG. 1. **Isolation and characterization of MAE-C57 and MAE-$p47^{-/-}$ cells.** *A*, C57BL/6 (C57) and $p47^{-/-}$ mice were genotyped by PCR using genomic DNA obtained from tail tissues. As a negative control, PCR was carried out in the absence of genomic DNA (*lane 3*). *B* and *C*, primary cultures obtained from thoracic aortas of C57Bl/6 and $p47^{-/-}$ mice were loaded with the endothelial marker DiI-Ac-LDL and sorted by a fluorescence activated cell sorter. Shown are fluorescence micrographs (10× magnification) of DiI-Ac-LDL-positive cells 2–3 h after plating on collagen-coated dishes (*B*) and cells photographed under a phase microscope (*C*). All cells shown are DiI-Ac-LDL-positive. *D*, some cells were stained with an endothelial cell marker, the von Willebrand factor (*vWF*), and a fluorescence-tagged secondary antibody and observed by fluorescence microscopy. *E*, cell lysates (20 μg each) obtained from wild type MAE and MAE-$p47^{-/-}$ were analyzed by immunoblot (*IB*) using a p47-specific antibody and actin (as a loading control). The *middle blank lane* contains molecular weight (*MW*) markers. Note that $p47^{phox}$ is expressed only in MAE-C57 cells but not in MAE-$p47^{-/-}$ cells. Shown are typical results of >10 separate isolation studies.

Both MAE-C57 and MAE-$p47^{-/-}$ cells aligned to the direction of imposed laminar shear (Fig. 2). Additional comparisons between the two MAE cell types showed that their exposure to LS

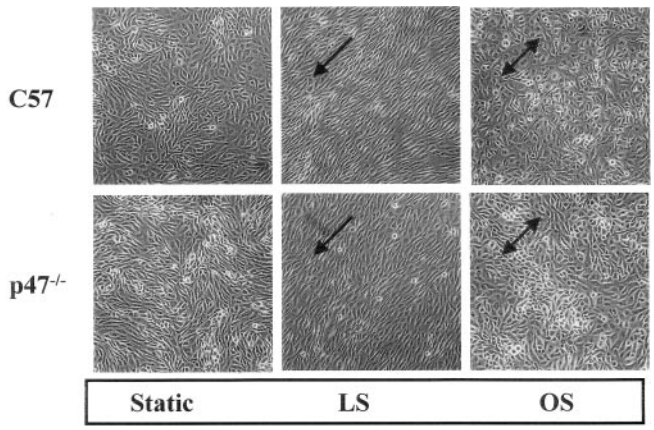

FIG. 2. **Cell alignment by LS, not by OS.** Confluent MAE-C57 and MAE-p47$^{-/-}$ monolayers grown in 100-mm plates were exposed to either static control, LS (15 dynes/cm^2), or OS (± 5 dynes/cm^2) using a cone-and-plate system for 24 h. Following shear exposure, cells were photographed under a phase microscope. Shown are typical cell shapes observed in >50 experiments each. Although shear exposure aligns both MAE-C57 and MAE-p47$^{-/-}$ cells to the direction of laminar flow, this effect was absent in oscillatory sheared MAEC. A typical cobblestone pattern at confluence is shown in the static conditions of MAE-C57 and MAE-p47$^{-/-}$, respectively.

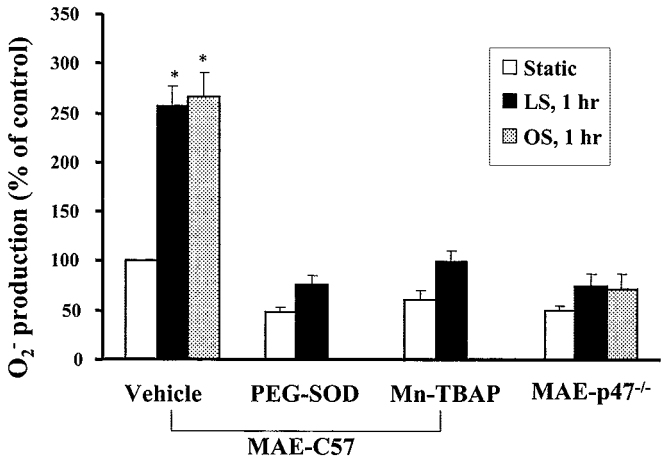

FIG. 3. **Superoxide production by LS or OS can be inhibited by either PEG-SOD, mangnese-TBAP, or p47^{phox} gene knockout.** Confluent MAE-C57 monolayers were exposed to either laminar (15 dynes/cm^2) or oscillatory shear (± 5 dynes/cm^2) for 1 h. Some cells were pre-treated with cell-permeable superoxide dismutase PEG-SOD (300 units/ml, 16 h) or a SOD mimetic manganese-TBAP (100 μM, 1 h) before shear onset. To examine whether superoxide was produced from NAD(P)H oxidase, MAE-p47$^{-/-}$ monolayers were exposed to static, LS, or OS conditions as described above. Immediately following shear, cells were incubated with 10 μM DHE for 10 min. After changing to fresh buffer, fluorescence images of cells at random positions representing O_2^- production were taken, and the fluorescence intensity was quantified (mean ± S.E., $n = 3$ to 4; *, $p < 0.01$).

stimulated phosphorylation of p42/p44 mitogen-activated protein kinases (extracellular signal-regulated kinase 1/2) and Akt (two well known shear-dependent signaling proteins) in a similar time course pattern with similar fold stimulations (data not shown). Moreover, as expected, neither MAE cell type displayed any signs of alignment when exposed to oscillatory shear (Fig. 2). These results suggest that both MAE cells respond in an expected manner to align to the imposed shear conditions and that the p47^{phox} gene product does not alter this morphological response.

Differential Effects of LS and OS on O_2^- Production from NAD(P)H Oxidase—Here, we examined whether relatively short (1–2 h) or long-term (18–24 h) exposure of endothelial cells to LS or OS regulates O_2^- production from NAD(P)H oxidases. We initially used an immunocytochemical method using DHE as an indicator of intracellular O_2^- production. Acute exposure of MAE-C57 cells to either LS or OS for a short period (1 h) significantly increased O_2^- production by 2.5-fold above static controls (Fig. 3). This result is consistent with previous findings (14). To ascertain the specificity of O_2^- production, MAE-C57 cells were treated with a cell-permeable SOD (PEG-SOD) or a SOD mimetic (manganese-TBAP). Both reagents substantially prevented O_2^- production in response to shear (Fig. 3). These results suggest that acute exposure of MAE-C57 cells to either LS or OS stimulated O_2^- production to a similar degree. We next examined whether this ROS was produced from NAD(P)H oxidases. To this end, we exposed MAE-p47$^{-/-}$ cells to LS or OS for 1 h and determined O_2^- production by DHE staining. In static conditions, MAE-p47$^{-/-}$ cells produced approximately half the amount of O_2^- compared with that of MAE-C57 cells (Fig. 3). More importantly, neither LS nor OS exposure was able to stimulate O_2^- production in MAE-p47$^{-/-}$ (Fig. 3). These results clearly suggest that short-term exposure of MAE-C57 cells to LS or OS stimulate ROS production, most likely O_2^-, from p47^{phox}-dependent NAD(P)H oxidases.

To assess shear stress-stimulated production of O_2^- in a more specific and quantitative manner, we used ESR. CMH was used as an O_2^--specific spin trap, and PEG-SOD-inhibitable formation of CM$^{\cdot}$ was determined. As shown above using the DHE staining assay, acute exposure (1 h) of MAE-C57 cells to LS or OS again stimulated O_2^- production by ~70% over that of static controls (Fig 4*B*). We also confirmed that MAE-p47$^{-/-}$ cells produced <50% of O_2^- in static cells and that both LS and OS failed to acutely stimulate these cells to produce more O_2^- (Fig. 4*B*).

Next, we examined the long-term effects on O_2^- production of exposing endothelial cells to LS or OS. MAE-C57 cells exposed to prolonged OS continued to produce ~75% more O_2^- than static conditions, whereas chronic LS exposure substantially inhibited O_2^- production by 70% below the static control (Fig. 4*C*). The chronic effect of OS on O_2^- production becomes even more impressive if we compare it to that of LS at 18 h. Chronic OS induced almost 6-fold increase in O_2^- production compared with that of LS (Fig. 4*C*). O_2^- production in MAE-p47$^{-/-}$ cells again showed no significant change in response to either LS or OS (Fig. 4*C*).

We further examined whether p47^{phox}-dependent NAD(P)H oxidases were responsible for shear-regulated O_2^- production by using a highly specific ESR method. In this study, MAE-C57 cells were pretreated with apocynin (600 μM), which inhibits a NAD(P)H oxidase by blocking the translocation of p47^{phox} to its membrane for 24 h prior to shear exposure (23), and O_2^- production was measured by ESR. Consistent with the DHE result shown in Fig. 4, chronic OS exposure increased O_2^- production by ~2-fold, which was virtually prevented by apocynin treatment (Fig. 5). This result further supports the notion that p47^{phox}-dependent endothelial NAD(P)H oxidases play a critical role in shear-induced O_2^- production.

In addition, these results demonstrate that different types of shear stress determine the duration of O_2^- produced by endothelial NAD(P)H oxidases. LS exposure induced a transient stimulation of O_2^- production during the first 1–2 h, followed by a significantly blunted long-term response (18–24 h). In contrast, OS exposure induced sustained levels of endothelial O_2^- production for the duration of the shear exposure. The inability of MAE-p47$^{-/-}$ cells to produce O_2^- in response to shear demonstrates a critical role of p47^{phox}-dependent NAD(P)H oxidase as the mechanosensitive source of ROS production.

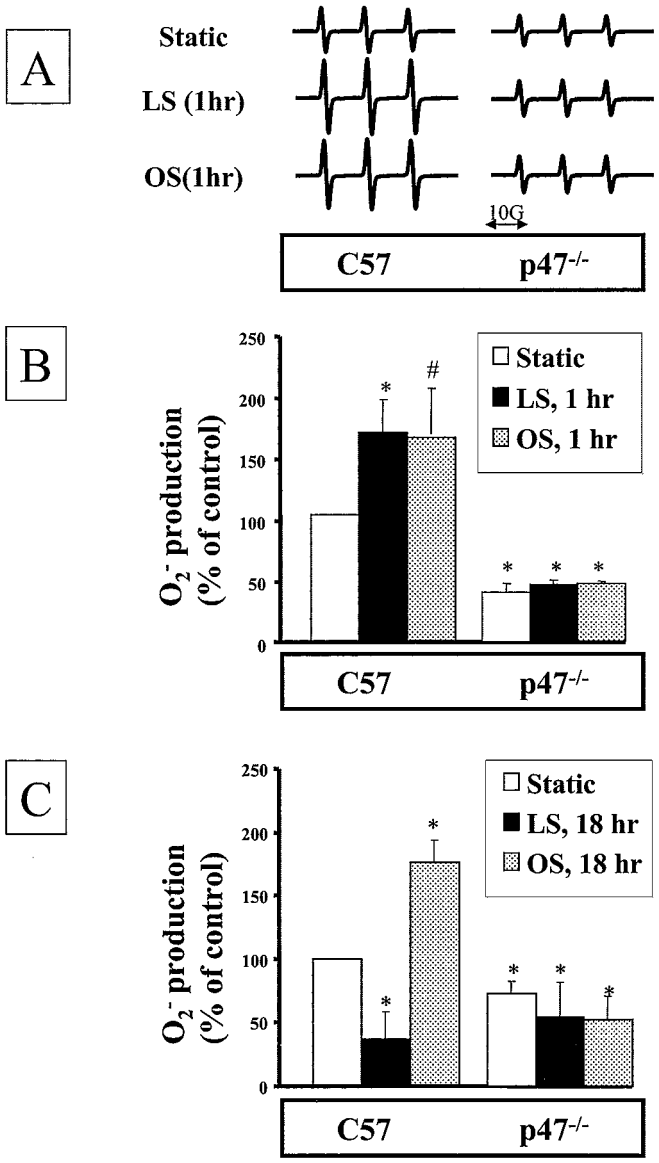

FIG. 4. **Superoxide production by LS or OS determined by ESR spectroscopy in MAE-C57 and MAE-p47$^{-/-}$.** Confluent MAE-C57 monolayers were exposed to laminar shear (15 dynes/cm2), oscillatory shear (± 5 dynes/cm2), or static conditions for 1 h (*A* and *B*) or 18 h (*C*). Immediately following shear, cells were scraped and centrifuged. An equal number of cells was incubated with a superoxide-specific spin trap CMH in the presence or absence of PEG-SOD (50 units/ml). Shown in *panel A* are representative superoxide spectra. For quantification, a time scan of CPH oxidation was obtained, and the slope was used as a measure of superoxide production. The *bar graphs* shown in *panels C* and *D* were calculated by subtracting SOD-inhibitable portions from total superoxide production (mean ± S.E., $n = 3$–4 each; #, $p < 0.05$; *, $p < 0.01$). Note that acute (1 h) exposure of MAE-C57 cells to either LS or OS increased the production of O_2^- to a similar degree. In contrast, chronic exposure of MAE-C57 to LS and OS inhibited and increased, respectively, O_2^- production. Unlike MAE-C57 cells, O_2^- production in MAE-p47$^{-/-}$ was substantially inhibited in static conditions, and neither LS nor OS stimulated O_2^- production above the control level.

NAD(P)H Oxidase-dependent Induction of Monocyte Adhesion by OS—Thus far our results demonstrate that shear stress stimulates O_2^- production from NAD(P)H oxidases. To determine whether the ROS produced from NAD(P)H oxidase in response to shear stress plays a critical role in endothelial function, we chose to study monocyte adhesion. First, we examined whether chronic exposure of endothelial cells to LS and OS affected monocyte binding. Chronic exposure of MAE-C57 cells to LS substantially inhibited monocyte binding by 50%

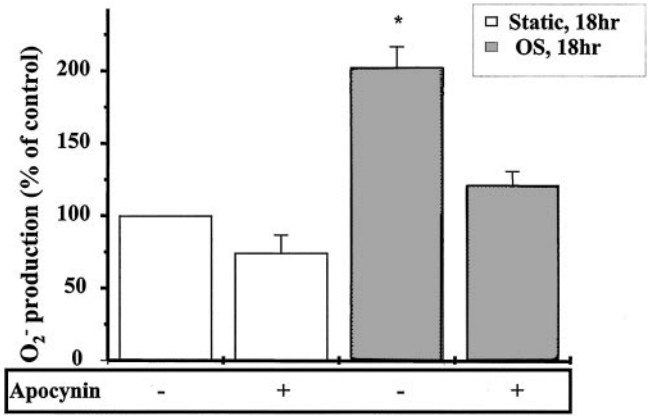

FIG. 5. **Apocynin, an NAD(P)H oxidase inhibitor, blocks OS stimulated O_2^- production in MAE-C57 cells.** Confluent MAE-C57 monolayers were exposed to 18 h of OS or static conditions as in Fig. 4 in the presence or absence of the NAD(P)H oxidase inhibitor apocynin (600 μM). Following shear or static treatment, O_2^- production in MAE-cells was measured by employing ESR in a manner described in the Fig. 4 legend. Note that chronic OS stimulated O_2^- production, which was inhibited by apocynin treatment.

compared with static conditions, whereas chronic OS significantly stimulated monocyte adhesion by almost 3-fold (Fig. 6). Treatment of MAE-C57 cells with an NAD(P)H oxidase inhibitor, apocynin (23), prevented OS-induced monocyte adhesion (Fig. 6), supporting a role for NAD(P)H oxidases in OS-induced monocyte binding. In contrast, apocynin did not alter the inhibitory effect of LS on monocyte adhesion, raising a speculation that p47^{phox}-dependent NAD(P)H oxidases play a role in OS-induced monocyte adhesion.

To further ascertain the role of p47^{phox}-dependent NAD(P)H oxidases in monocyte binding, we compared shear regulated monocyte adhesion of MAE-C57 to that of MAE-p47$^{-/-}$ cells. In support of our hypothesis, we found that monocyte binding to MAE-p47$^{-/-}$ cells under static conditions was ~50% lower than that to MAE-C57 cells (Fig. 7). Furthermore, unlike MAE-C57 cells, chronic exposure (18 h) of MAE-p47$^{-/-}$ to LS or OS did not significantly affect monocyte adhesion (Fig. 7). This result is consistent with the apocynin effects shown in Fig. 5 and confirms the critical role of p47^{phox}-dependent NAD(P)H oxidase in shear-induced monocyte adhesion. It is interesting to note that O_2^- production in the MAE-p47$^{-/-}$ cells is decreased by ~50% as well (Fig. 4).

Next, we examined the time dependence of LS and OS effects on monocyte adhesion. Exposure of MAE-C57 cells to 4 h of LS was enough to inhibit monocyte adhesion (Fig. 7). However, 4 h of OS failed to stimulate monocyte adhesion in MAE-C57 cells (Fig. 7). As expected, LS or OS exposure of MAE-p47$^{-/-}$ for 4 h had no significant effect on monocyte adhesion (Fig. 7). These findings indicate that OS-induced monocyte adhesion requires a chronic shear exposure longer than 18 h, whereas 4 h of LS exposure is enough to cause inhibition of monocyte adhesion as reported perviously (22).

O_2^- Produced from p47^{phox}-dependent NAD(P)H Oxidases Is Responsible for OS-induced Monocyte Adhesion to Endothelial Cells—To date, we have shown that OS induces monocyte adhesion in MAE-C57 cells. To confirm that these effects are a consequence of altering the superoxide level, we examined whether monocyte binding to MAE cells can be blocked by either treating cells with cell-permeable SOD or transfecting them with p47^{phox} cDNA. First, we treated MAE-C57 cells with a cell-permeable PEG-SOD to determine whether the removal of intracellular O_2^- would inhibit the OS-induced monocyte binding response. Treatment of MAE-C57 cells with PEG-SOD did indeed block monocyte adhesion to static control levels (Fig. 8).

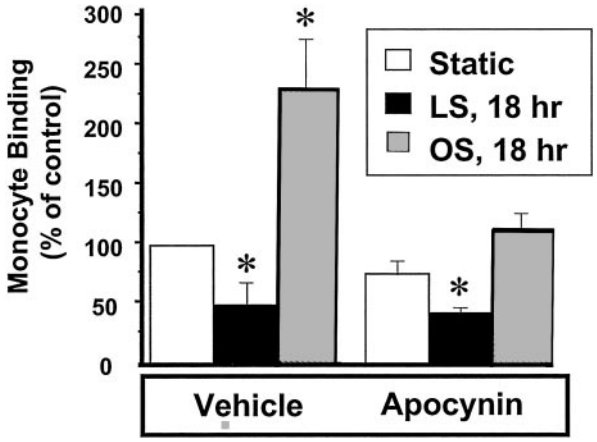

FIG. 6. **Chronic exposure of MAE-C57 to LS and OS inhibits and stimulates monocyte adhesion in an apocynin-dependent manner.** Confluent MAE-C57 monolayers were exposed to 18 h of LS, OS, or static conditions as in Fig. 4 in the presence or absence of a NAD(P)H oxidase inhibitor apocynin (600 μM). Following shear or static treatment, MAE cells were washed and incubated with fluorescently labeled THP-1 monocytes. After 30 min, unbound cells were washed away, the bound monocytes were lysed, and the fluorescence intensity was determined by fluorescence spectroscopy. The result shown represents mean ± S.E. (*, $p < 0.05$; $n = 6$). Note that chronic LS inhibited and OS stimulated monocyte binding, which was blocked by apocynin treatment.

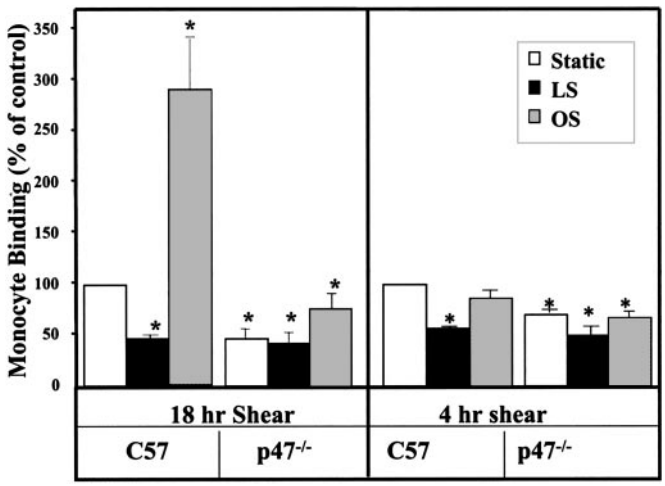

FIG. 7. **p47^{phox} gene knockout blocks monocyte adhesion induced by chronic OS exposure of endothelial cells.** Confluent MAE-C57 and MAE-p47$^{-/-}$ monolayers were exposed to LS, OS, or static controls for either 18 or 4 h as described in the Fig. 4 legend. Following shear exposure, monocyte adhesion was determined as described in the Fig. 6 legend. Shown are means ± S.E. (*, $p < 0.05$; $n = 6$). Note that monocyte adhesion to MAE-p47$^{-/-}$ cells in static as well as OS exposure were considerably blocked. It is also noted that exposure to OS for a relatively short time (4 h) failed to induce monocyte adhesion.

Next, MAE-p47$^{-/-}$ cells were transfected with the cDNA vector encoding p47^{phox} protein or an empty vector control. First, we verified that p47^{phox} transfection indeed resulted in over-expression of the 47-kDa protein by Western blot analysis by using a p47^{phox}-specific antibody (Fig 9*A*). Next, we found that the MAE-p47$^{-/-}$ cells transfected with p47^{phox} responded to OS by producing O_2^- by >2-fold above the static cells (Fig. 9*B*). Finally, as shown in Fig. 9*C*, we were able to restore monocyte adhesion in response to chronic OS by over-expressing p47^{phox} protein in MAE-p47$^{-/-}$ cells. In contrast, OS exposure of MAE-p47$^{-/-}$ cells transfected with the empty vector did not increase monocyte adhesion nearly as much as that of p47^{phox}-transfected cells. The OS-induced monocyte adhesion was completely inhibited by the NAD(P)H oxidase inhibitor, apocynin (Fig. 9*C*), providing further evidence for the specific of effect of p47^{phox}.

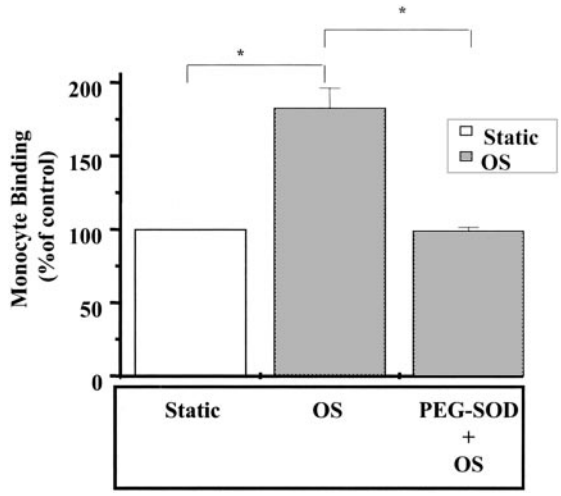

FIG. 8. **Effects of PEG-SOD, an intracellular superoxide-scavenging compound, on OS-induced monocyte adhesion to MAE-C57 cells.** Confluent MAE-C57 monolayers were exposed to 18 h of LS, OS, or static conditions as in Fig. 4 in the presence or absence of the O_2^- scavenger PEG-SOD (300units/ml). Following shear exposure, monocyte adhesion was determined as described in the Fig. 6 legend. Shown are means ± S.E. (*, $p < 0.05$; $n = 6$). Note that chronic OS-stimulated monocyte binding was inhibited by PEG-SOD treatment.

DISCUSSION

The most significant and interesting findings of the current study are that chronic exposure of endothelial cells to OS stimulates O_2^- production and monocyte adhesion by p47^{phox}-dependent, NAD(P)H oxidase-derived mechanisms requiring O_2^- or its ROS derivatives. Previous studies have shown that shear stress stimulates production of ROS and reactive nitrogen species (13, 14). Our current results strongly suggest that shear stress induces O_2^- production from endothelial cells. Several lines of evidence presented below support this conclusion. First, treatment of MAE-C57 cells with a cell-permeable SOD (PEG-SOD) and a SOD mimetic (manganese-TBAP) inhibited O_2^- produced by shear stress. Second, O_2^- production was determined by using two independent methods, DHE staining and ESR using CMH as a spin probe. In addition, ESR measurements were carried out in the presence or absence of PEG-SOD to determine the SOD-inhibitable portion of O_2^- production. This second approach provided clear specificity for O_2^- measurement.

ROS can be produced in the vasculature from several sources, including membrane and mitochondrial NAD(P)H oxidases, cytochrome P450, xanthine oxidase, and uncoupled nitric oxide synthase (9). Overwhelming evidence now suggests that non-mitochondrial NAD(P)H oxidases are a major source of ROS in vascular smooth muscle cells and endothelial cells (9). The endothelial NAD(P)H oxidase is believed to be similar to the leukocyte NAD(P)H oxidase, and several of its components have been identified, including p47^{phox}, p67^{phox}, Rac, p22^{phox}, and gp91^{phox} (9, 24). Recently, several members of gp91^{phox} homologues (referred to as the "Nox" family) were identified (25, 26). In endothelial cells, it appears that Nox 4 is the most abundant member, whereas Nox 1 and gp91^{phox} (currently designated as Nox 2) have also been detected at low levels (27).

Although it has been suggested that NAD(P)H-dependent oxidases are activated by shear stress (14), the extent of its involvement in shear-induced O_2^- production was not clear. Our current results strongly indicate that the major source of

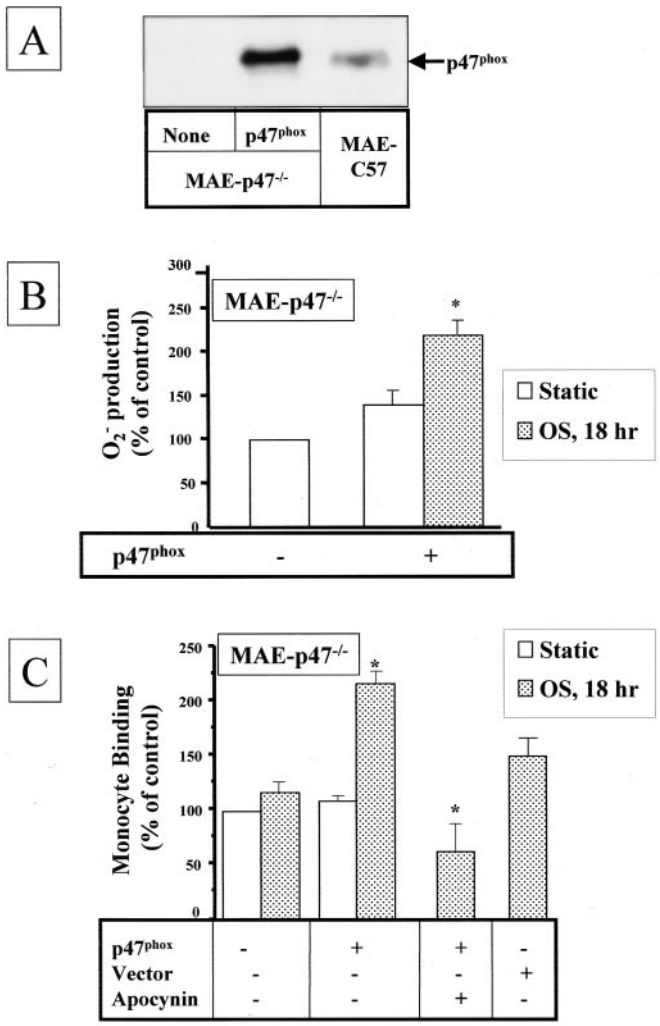

FIG. 9. **Chronic OS induces monocyte adhesion to MAE-p47$^{-/-}$ cells transfected with p47^{phox} vector.** MAE-p47$^{-/-}$ cells were transfected with p47^{phox} vector or empty vector control (*Vector*) by using LipofectAMINE. *A*, 1 day after transfection, cell lysates were obtained and analyzed by Western blot using a p47-specific antibody. Cell lysates of MAE-C57 were used as controls. Shown is a representative of 3–6 different studies. *B* and C, 1 day after transfection, cells were exposed to OS or static control for 18 h. In some studies, apocynin (600 μM) was added during shear. Then, O_2^- production was measured by ESR (*B*) as described in the Fig. 4 legend or monocyte adhesion was determined as described above (*C*). The *bar graphs* shown in *panels B* and *C* are the means ± S.E., $n = 6$; *, $p < 0.05$.

endothelial O_2^- produced in response to shear stress is p47^{phox}-dependent endothelial NAD(P)H oxidase. This conclusion is based on the following observations. First, treatment of MAE-C57 cells with apocynin inhibited shear-dependent O_2^- production, suggesting a role for NAD(P)H oxidases activated by the translocation of cytosolic subunits. Second, MAE-p47$^{-/-}$ cells failed to produce O_2^- in response to either chronic or acute LS and OS exposure. Third, over-expression of wild type p47^{phox} protein in MAE-p47$^{-/-}$ cells restored OS-induced production of O_2^-, further demonstrating the critical role of p47^{phox}-dependent NAD(P)H oxidases as a major source of mechanosensitive ROS production. Although the role of a p47^{phox}-dependent NAD(P)H oxidase is clear, it is not known which Nox (Nox 1, 2 and 4) is responsible for shear-dependent O_2^- production in endothelial cells.

We found that O_2^- production in response to LS was transiently regulated, whereas OS induced continuous O_2^- production at higher (4-fold) levels compared with LS. Short-term exposure (1–2 h) to LS and OS resulted in similar levels of O_2^- production. The mechanisms responsible for this differential shear type-dependent and time-dependent O_2^- production are not clear at this point. Several known mechanisms, however, could explain this. First, consistent to previous findings (28–30), we have found that chronic LS stimulated a significantly higher level of NO production in comparison to OS (data not shown). NO is a potent antioxidant and binds O_2^-, which would decrease its detectable levels (21). The shift in balance from "high NO and low O_2^-" in LS-conditioned cells to "low NO and high O_2^-" by OS may be an important factor contributing to a pro-atherogenic response such as monocyte adhesion. Second, LS and OS could differentially regulate expression of other antioxidant enzymes in a time-dependent manner. For example, LS but not turbulent or OS has been shown to induce numerous antioxidant enzymes such as copper/zinc-SOD (14, 31), heme oxygenase-1 (14), manganese-SOD (32), and glutathione peroxidase (33). Third, it is possible that LS and OS may differentially regulate activity and expression levels of NAD(P)H oxidases. Consistent with this possibility, atherosclerotic lesions, which typically occur in arterial regions exposed to disturbed shear conditions, contain higher levels of ROS and NAD(P)H oxidase components, including Nox2, Nox4, and p22^{phox} (27). Taken together, we propose that the balance between O_2^- production and antioxidants is determined by the duration and type of shear imposed on endothelial cells. In the short term, other than endothelial nitric oxide synthase, the expression and activation of other anti-oxidant enzymes may not be sufficient to counter the O_2^- produced in response to LS and OS. On the other hand, chronic exposure to LS induces enough antioxidants to blunt O_2^- production, whereas OS may either decrease or have no effect on antioxidant levels.

We found that while prolonged (18 h) exposure of endothelial to OS induced monocyte adhesion, acute (4 h) OS did not (Fig. 7), raising a possibility that OS-dependent monocyte adhesion requires new gene synthesis. These results are consistent with the recent finding that chronic OS exposure of endothelial cells stimulates bone morphogenic protein-4 expression, which then leads to monocyte adhesion by inducing intercellular adhesion molecule-1 in a NFκB-dependent manner (7). In addition, OS has been shown to stimulate monocyte adhesion in an *N*-acetylcysteine-inhibitable manner (8). Although this finding suggested a role for ROS in OS-induced monocyte adhesion, its identity and source were not known. Based on our current study, it is now clear that the shear-induced O_2^- and its derivatives being produced in endothelial cells are derived from NAD(P)H oxidases. Furthermore, we conclude that O_2^- and its derivatives produced from NAD(P)H oxidase are responsible for monocyte adhesion induced by OS.

It is not clear at this point, however, whether O_2^- and/or its derivatives (*e.g.* H_2O_2 and $ONOO^-$) are responsible for the OS-dependent monocyte adhesion. Our results suggest that OS-induced monocyte adhesion may occur through multiple pathways acting in concert, one of which is O_2^--dependent. Treatment of cells with PEG-SOD resulted in a significant inhibition of OS-mediated monocyte adhesion in MAE-C57 cells.

Atherosclerosis is a focal, inflammatory disease preferentially occurring at lesion-prone areas exposed to unstable shear stress (3). Although LS has been shown to induce anti-inflammatory, atheroprotective responses, OS has been associated with pro-inflammatory and pro-atherogenic responses (4, 5). Whereas these previous studies (8) have suggested a connection between OS, ROS, and monocyte adhesion, the identity and source of ROS and its functional significance have not been clearly demonstrated. Using MAE cells obtained from C57 and p47$^{-/-}$ mice and employing ESR spectroscopy and monocyte

adhesion assays, here we have determined the identity and source of ROS and its direct role in monocyte adhesion in response to shear stress. In summary, we have identified O_2^- as being produced from endothelial NAD(P)H oxidases in response to shear stress and have shown that this ROS and its derivatives are directly responsible for monocyte adhesion, a critical step in atherogenesis.

Acknowledgment—We thank Dr. Bernard Babior for providing the $p47^{phox}$ vector.

REFERENCES

1. Zarins, C. K., Giddens, D. P., Bharadvaj, B. K., Sottiurai, V. S., Mabon, R. F., and Glagov, S. (1983) *Circ. Res.* **53,** 502–514
2. Ku, D. N., Giddens, D. P., Zarins, C. K., and Glagov, S. (1985) *Arteriosclerosis* **5,** 293–302
3. Ross, R. (1999) *N. Engl. J. Med.* **340,** 115–126
4. Berk, B. C., Abe, J. I., Min, W., Surapisitchat, J., and Yan, C. (2001) *Ann. N. Y. Acad. Sci.* **947,** 93–111
5. Davies, P. F. (1995) *Physiol. Rev.* **75,** 519–560
6. Garcia-Cardena, G., Comander, J., Anderson, K. R., Blackman, B. R., and Gimbrone, M. A., Jr. (2001) *Proc. Natl. Acad. Sci. U. S. A.* **98,** 4478–4485
7. Sorescu, G. P., Sykes, M., Weiss, D., Platt, M. O., Saha, A., Hwang, J., Boyd, N., Boo, Y. C., Vega, J. D., Taylor, W. R., and Jo, H. (2003) *J. Biol. Chem.* **278,** 31128–31135
8. Chappell, D. C., Varner, S. E., Nerem, R. M., Medford, R. M., and Alexander, R. W. (1998) *Circ. Res.* **82,** 532–539
9. Griendling, K. K., Sorescu, D., and Ushio-Fukai, M. (2000) *Circ. Res.* **86,** 494–501
10. Patel, R. P., Moellering, D., Murphy-Ullrich, J., Jo, H., Beckman, J. S., and Darley-Usmar, V. M. (2000) *Free Radic. Biol. Med.* **28,** 1780–1794
11. Babior, B. M. (2002) *Isr. Med. Assoc. J.* **4,** 1023–1024
12. Landmesser, U., Cai, H., Dikalov, S., McCann, L., Hwang, J., Jo, H., Holland, S. M., and Harrison, D. G. (2002) *Hypertension* **40,** 511–515
13. Go, Y. M., Patel, R. P., Maland, M. C., Park, H., Beckman, J. S., Darley-Usmar, V. M., and Jo, H. (1999) *Am. J. Physiol.* **277,** H1647–H1653
14. De Keulenaer, G. W., Chappell, D. C., Ishizaka, N., Nerem, R. M., Alexander, R. W., and Griendling, K. K. (1998) *Circ. Res.* **82,** 1094–1101
15. Jackson, S. H., Gallin, J. I., and Holland, S. M. (1995) *J. Exp. Med.* **182,** 751–758
16. Suh, S. H., Vennekens, R., Manolopoulos, V. G., Freichel, M., Schweig, U., Prenen, J., Flockerzi, V., Droogmans, G., and Nilius, B. (1999) *Pfluegers Arch. Eur. J. Physiol.* **438,** 612–620
17. Go, Y. M., Park, H., Maland, M. C., Darley-Usmar, V. M., Stoyanov, B., Wetzker, R., and Jo, H. (1998) *Am. J. Physiol.* **275,** H1898–H1904
18. Jo, H., Sipos, K., Go, Y. M., Law, R., Rong, J., and McDonald, J. M. (1997) *J. Biol. Chem.* **272,** 1395–1401
19. Szocs, K., Lassegue, B., Sorescu, D., Hilenski, L. L., Valppu, L., Couse, T. L., Wilcox, J. N., Quinn, M. T., Lambeth, J. D., and Griendling, K. K. (2002) *Arterioscler. Thromb. Vasc. Biol.* **22,** 21–27
20. Zhao, H., Kalivendi, S., Zhang, H., Joseph, J., Nithipatikom, K., Vasquez-Vivar, J., and Kalyanaraman, B. (2003) *Free Radic. Biol. Med.* **34,** 1359–1368
21. Kuzkaya, N., Weissmann, N., Harrison, D. G., and Dikalov, S. (2003) *J. Biol. Chem.* **278**, 22546–22554
22. Tsao, P. S., Buitrago, R., Chan, J. R., and Cooke, J. P. (1996) *Circulation* **94,** 1682–1689
23. Holland, J. A., O'Donnell, R. W., Chang, M. M., Johnson, D. K., and Ziegler, L. M. (2000) *Endothelium* **7,** 109–119
24. Li, J. M., and Shah, A. M. (2002) *J. Biol. Chem.* **277,** 19952–19960
25. Suh, Y. A., Arnold, R. S., Lassegue, B., Shi, J., Xu, X., Sorescu, D., Chung, A. B., Griendling, K. K., and Lambeth, J. D. (1999) *Nature* **401,** 79–82
26. Lambeth, J. D., Cheng, G., Arnold, R. S., and Edens, W. A. (2000) *Trends Biochem. Sci.* **25,** 459–461
27. Sorescu, D., Weiss, D., Lassegue, B., Clempus, R. E., Szocs, K., Sorescu, G. P., Valppu, L., Quinn, M. T., Lambeth, J. D., Vega, J. D., Taylor, W. R., and Griendling, K. K. (2002) *Circulation* **105,** 1429–1435
28. Ziegler, T., Silacci, P., Harrison, V. J., and Hayoz, D. (1998) *Hypertension* **32,** 351–355
29. Boo, Y. C., Sorescu, G., Boyd, N., Shiojima, I., Walsh, K., Du, J., and Jo, H. (2002) *J. Biol. Chem.* **277,** 3388–3396
30. Boo, Y. C., Hwang, J., Sykes, M., Michell, B. J., Kemp, B. E., Lum, H., and Jo, H. (2002) *Am. J. Physiol.* **283,** H1819–H1828
31. Dimmeler, S., Hermann, C., Galle, J., and Zeiher, A. M. (1999) *Arterioscler. Thromb. Vasc. Biol.* **19,** 656–664
32. Topper, J. N., Cai, J., Falb, D., and Gimbrone, M. A., Jr. (1996) *Proc. Natl. Acad. Sci. U. S. A.* **93,** 10417–10422
33. Takeshita, S., Inoue, N., Ueyama, T., Kawashima, S., and Yokoyama, M. (2000) *Biochem. Biophys. Res. Commun.* **273,** 66–71
34. Endres, M., Laufs, U., Merz, H., and Kaps, M. (1997) *Stroke* **28,** 77–82
35. Libby, P., Ridker, P. M., and Maseri, A. (2002) *Circulation* **105,** 1135–1143
36. Cybulsky, M. I., Iiyama, K., Li, H., Zhu, S., Chen, M., Iiyama, M., Davis, V., Gutierrez-Ramos, J. C., Connelly, P. W., and Milstone, D. S. (2001) *J. Clin. Invest.* **107,** 1255–1262